Assessing the tunnel stability in brittle rocks based on strain bursting assessment

Assessing the tunnel stability in brittle rocks based on strain bursting assessment

Lans Aujmaya[1], Ioannis Vazaios[2], Chrysothemis Paraskevopoulou[1]*

[1]School of Earth and Environment, University of Leeds, Leeds, United Kingdom
[2]Ove Arup & Partners Ltd, London, United Kingdom

*c.paraskevopoulou@leeds.ac.uk

Abstract. Strain bursting is a phenomenon associated with deep underground excavations and tunnelling in brittle hard rocks that result in a sudden and violent failure, posing high risks and damage. This work aims to assess the strain bursting and the energy response characteristics and develop a guideline that can be utilized in the preliminary investigation stage. The obtained results are intended to enable predicting different brittle behaviours in deep geological environments. Elastic stress analysis using the DISL approach based on boundary element method is established (EX3-software) for the assessment of two tunnel geometries (circular, horseshoe) in granitic rock mass. Two different stress states are modelled to simulate the potential stress regime. The analysis' results demonstrate that different geometries affect the energy storage capacity and result in different behaviour regarding the bursting potential of the rock mass.

1. Introduction

Underground excavations and deep tunnelling in hard rock masses are carried out to host applications such as nuclear waste disposal facilities, storage, energy, transport infrastructure etc. providing solutions to many of today's world problems [1]. Historically, challenges associated with deep underground excavations pose significant risks and need to be considered before planning any underground construction. Strain bursting has become a more frequent phenomenon occurring in hard rock tunnelling and mining due to the high-stress magnitude and anisotropic conditions threatening the safety of the working personnel, the integrity of the excavation equipment and the overall tunnel stability due to its violent and sudden nature [2].

Many authors have investigated brittle failure in deep excavation and provided many empirical and semi-empirical relationships for predicting the damage zones, such as [2], [3], [4], [5] and others. In recent years, numerical modeling provided an easy and effective approach to model different phenomena including strain-bursting in a similar fashion and for the purpose of this research work, the Boundary Element Method (BEM) has been utilized. The paper aims to develop and present a simple and straight-forward approach for analyzing and assessing strain bursting at the preliminary stages of the design.

2. Background

Excavations in brittle rock masses in deep geological environments for mining or tunneling are associated with brittle fracturing which can be divided into two main categories depending on the nature of the failure, which are spalling and strain bursting [6]. Strain-bursting phenomenon occurs in

massive to moderately jointed rock masses with high Unconfined Compressive Strength (UCS) values [2]. [7] emphasize that the damage initiation in the low confinement zone of excavations and underground openings is controlled by the evolution and propagation of extension fractures generated from stress concentrators such as microscopic cracks or discontinuities, grain boundaries, and non-persistent joints in a moderately jointed rock mass. These phenomena usually occur in crystalline rocks near excavation boundaries under high stress (Figure 1). [6] developed an approach to predict the susceptibility of rock spalling based on the ratio between the compressive to the tensile strength of the material and additionally he proposed a modified Hoek-Brown criterion predicting damage initiation and spalling limit (DISL) shown in Figure 1.

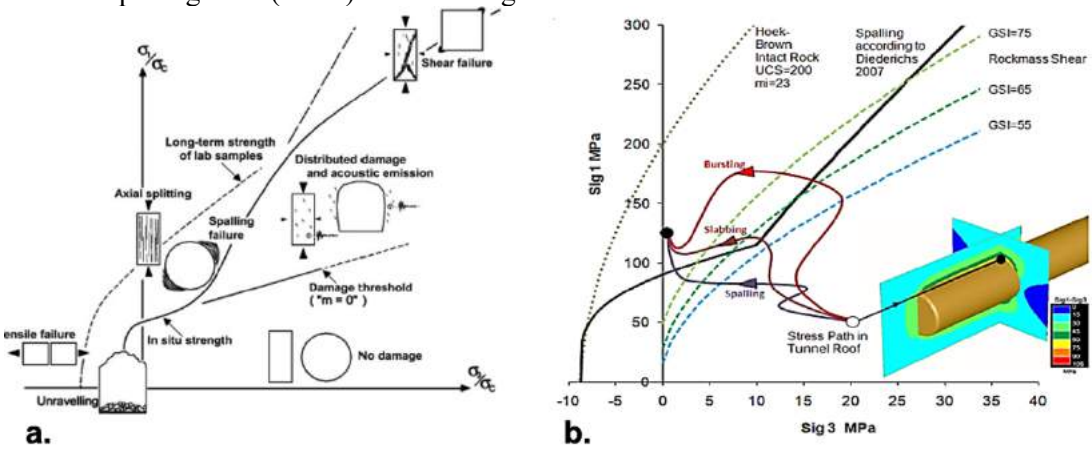

Figure 1. a. Schematic of failure envelope for brittle failure illustrating different zones of rock mass failure mechanisms [2]; and, b. Stress path approach for determining burst potential based on energy storage release [8].

3. Methodology

3.1. Boundary Element Method (BEM)

The BEM comprises partial differential equations for stress analysis by renovating this equation which can be defined as the representative of the behaviour of a given system throughout a volume to integral equations situated only on the boundary of the same system [9]. The BEM is applied for analysis for three primary reasons: (a) As the elastic behaviour of the rock bursting mechanism is only considered in this study (b) tunnels can be classified within the category of structural elements that functions in the plane strain state and (c) a homogenous rock mass will be modelled. EX3 software (Rocscience) uses BEM and provides a practical and powerful approach for elastic analysis of tunnels and underground excavations. EX3 is a simple platform that allows to import/export of complicated geometries easily, automatic surface meshing, and creation of field points in the shape of planes or boxes, and many other valuable features. In the following sections, the implementation of the numerical models is described in detail.

3.2. Rock Properties and Stress Conditions

For the purpose of this work a granitic rock mass is examined. The intact rock properties are listed in Table 1.a and are converted to rock mass properties using RocData software assuming a GSI of 85, which represents a blocky structure with good to very good surface conditions. which represents a blocky to massive structure with good to very good surface conditions. It is also assumed that the tunnel is excavated at 500 m depth with a stress ratio as shown in Table 1.b

Assuming such GSI is justified as an elastic analysis will be conducted, and the tunnel is being constructed at a depth of 500m.

Table 1. a. Rock properties and b. stress conditions after [10] and [11].

a. Rock type: Granite		
Young's Modulus (GPa)	Intact *(Ei)*	52
	Rock mass	48
Poisson's ratio ν (-)		0.4
Density, ρ (kg/m³)		2650
mi		31
Rock mass tensile strength, σt (MPa)		-1.397
Compressive strength (MPa)	Intact *(UCS)*	138.5
	Rock mass	60.15
b. Stress Conditions		
K-ratio	1	4
σv (MPa)	13.25	13.25
σh (MPa)	13.25	53

3.3. Model set-up

Two excavations geometries are considered herein for the analysis process, which allows to investigate and define the effects of different geometry on the behavior of the rock mass around the excavation. The geometries consist of a 7 m diameter circular tunnel and horseshoe with 5 m span and 5 m height. The total length of the tunnel is assumed to be 20 m and is created as a multi-stage model, consisting of 8 stages of 3 m advancement, assuming a drill and blast excavation method. Inductively the horseshoe excavation profile and sequence is shown in Figure 2 and Figure shows the approach used in the numerical analysis.

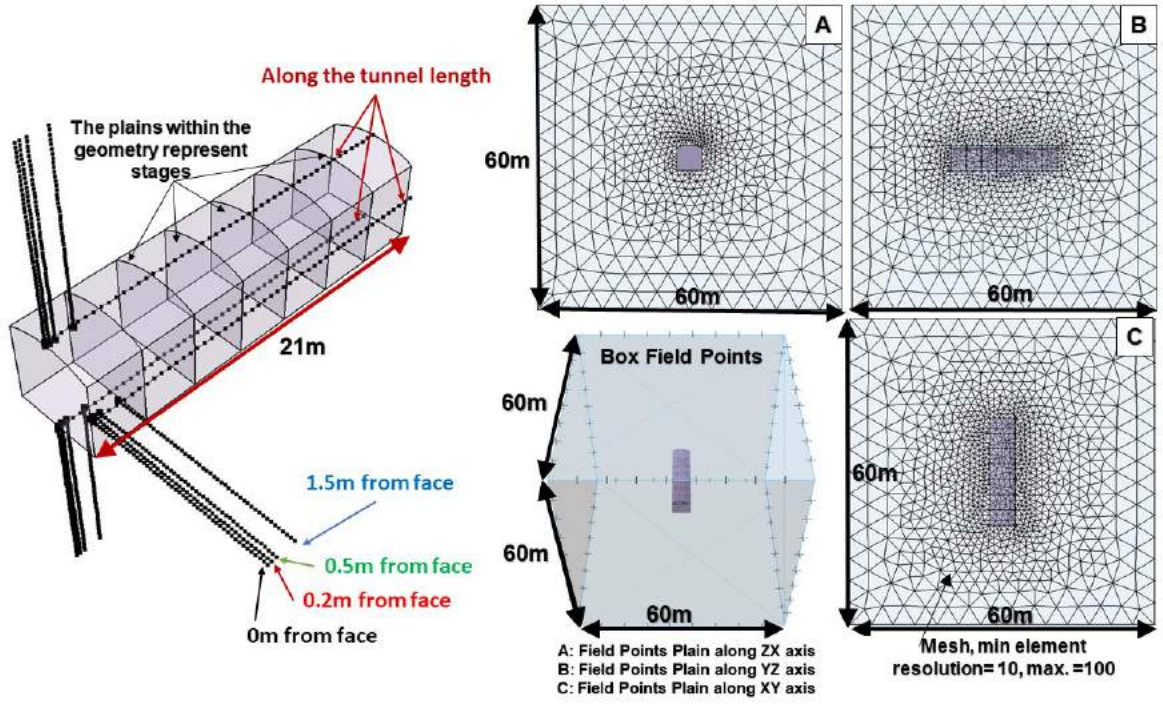

Figure 2. Schematic representation of the horseshoe excavation profile and sequence.

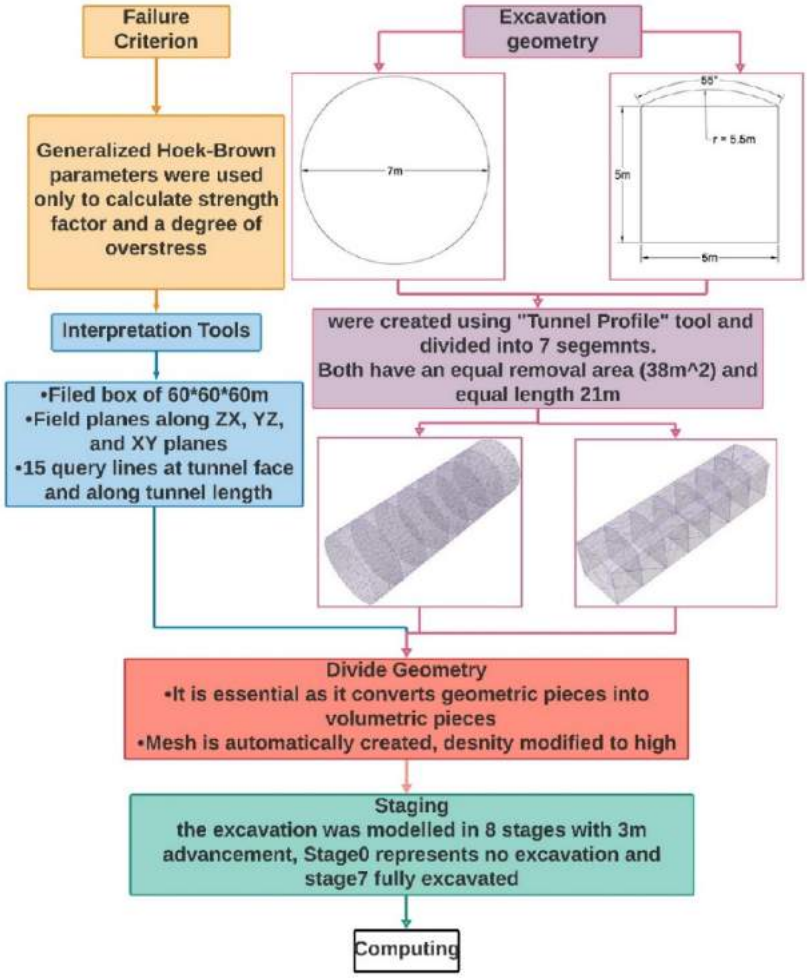

Figure 3. Flow chart representing the followed steps for the model development.

3.4. Material strength envelope

The damage initiation and spalling limit approach by [6], previously described, is herein used to predict damage initiation, and spalling for the granitic rock mass shown in Figure 4.

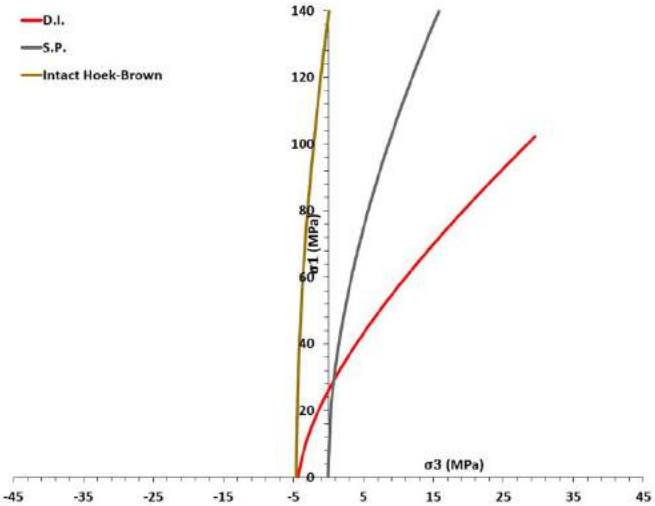

Figure 4. Damage initiation (D.I.), Spalling limit (S.P.), and intact Hoek-Brown envelopes for gneiss rock mass based on DISL models by [6].

4. Numerical Analysis and Results

4.1. Stress paths

A stress path is used to observe and represent the successive states of stress; the principal stresses (σ_1 and σ_3 are plotted on a normal scale graph (σ_1 on the vertical axis and σ_3 on the horizontal axis). Additionally, the strength envelopes as derived from DISL are also shown in the Figure 5. Stress paths are plotted at three locations along the tunnel length: the crown, the floor, and the sidewall. The measurements are taken from 3 m, 6 m, 9 m, 12 m, 15 m, and 18 m at seven stages to reflect an excavation advancement rate of 3 m and the stress increase at each point with staging. A general curve was drawn to illustrate the same observed path in single shared stress development at several points, and different curves were drawn if different stress paths were observed.

4.2. Depth of failure

The volume of the failed material is estimated to determine the elastic energy release at different stages of excavation advancement of the tunnel. The damage depth is determined using the strength factor around the tunnel geometry as evaluated from the elastic stresses divided by the strength envelope as obtained the DISL approach. The depth of failure is shown in Figure 6.

4.3. Elastic energy density calculations

An assessment evaluation of the stored elastic energy has been carried out following the calculations of principal strains using the stress values obtained from the numerical analysis. The average strain energy is estimates using Equation 1, where u is the average strain energy density, σ_i is the major principal stress and ε_i is the principal strain.

$$u = \frac{1}{2} * [(\sigma_1 * \varepsilon_1) + (\sigma_2 * \varepsilon_2) + (\sigma_3 * \varepsilon_3)] \qquad (1)$$

After deriving the elastic strain density, the elastic strain energy release of the ejected volume can be estimated by multiplying the elastic energy density by the volume of the ejected material estimated using the strength factor approach as shown in Equation 2, where U is the elastic energy release and Ve the ejected volume.

$$U = u * V_e \qquad (2)$$

The calculated energy release is plotted along the tunnel length and presented in Figure 7.

5. Discussion

Brittle failure can occur in hard rock masses with high compressive stress under high-stress conditions. Failure modes are observed in the numerical models analysed, primarily based on the difference in situ stress, tunnel geometry. At the crown, both geometries show damage initiation and cracking with no prominent spalling and slabbing at K=1 though the horseshoe tunnel shows a different stress path when measured at the point of 15 m. Granite rock mass shows bursting alone K= 4 with more energy storage for a circular tunnel. For the horseshoe tunnel, granite rock mass at K=4 shows slabbing for all points and bursting at point 15 m. Many researchers suggested that the failure occurs when the major principal stress ranges from 40% to 60% of the intact UCS [2], [8]. Comparing the depth of failure from the empirical formulas by [4], [12] with the numerically observed depth of the failure by the strength factor approach, it can be stated that the numerical models provide good precision at K equal to 4. The extent of failure estimated from the strength factor approach showed variations especially with different surfaces of the horseshoe tunnel. Having estimated the extent of damage, the calculated stored energy that is released occurs as the strength of the rock mass is exceeded, which abrupt in nature for the granitic rock mass. This however may be different for other rock mass types and further investigation is required. The geometrical variations between the tunnel profiles are also noted as the circular tunnel has a more defined behaviour than the horseshoe. Different surfaces of the horseshoe tunnel to store energy result in different energy storage capability

and thus in more energy release particularly in the case of the flat floor compared to the arc shaped crown.

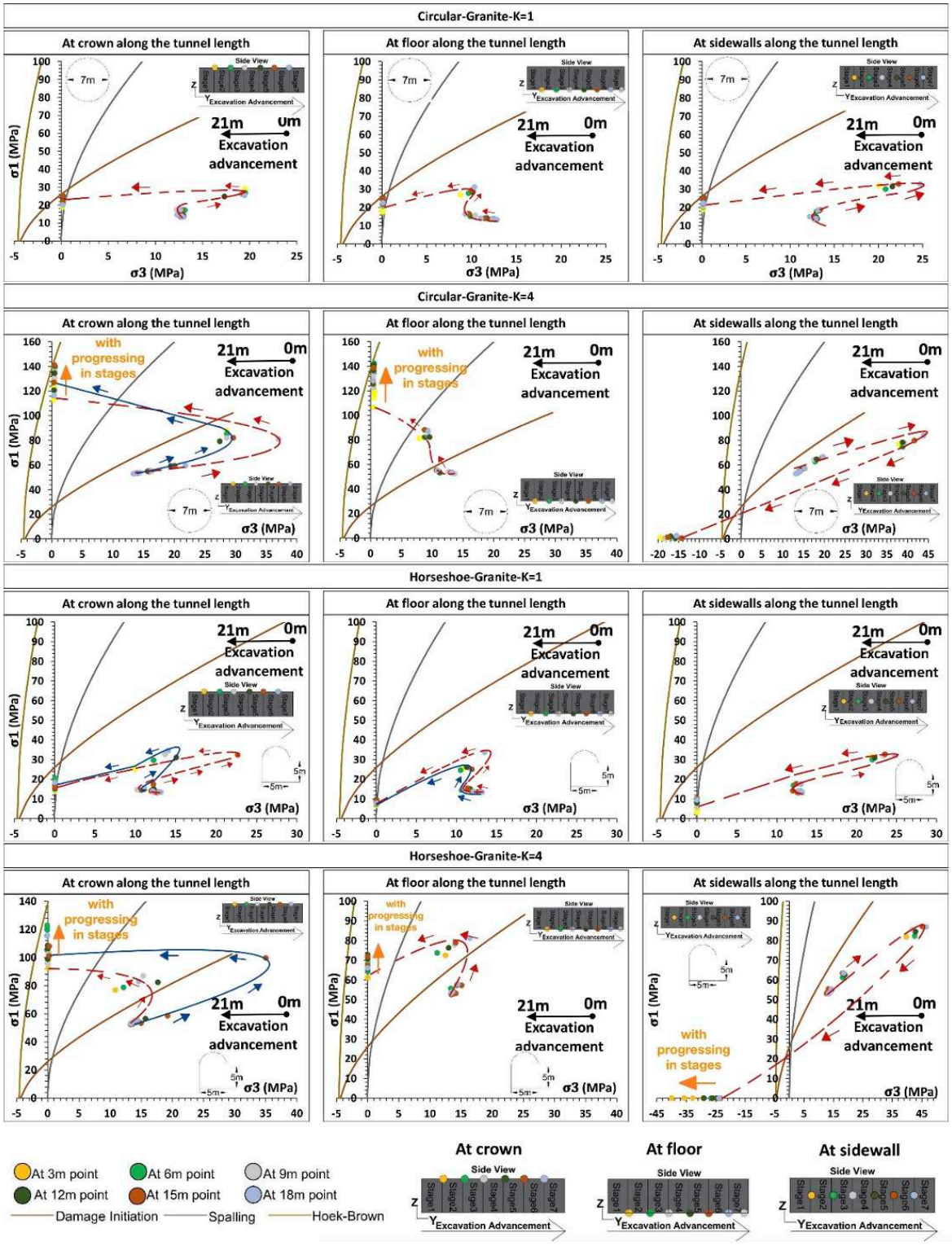

Figure 5. Stress paths represented by the values of the principal stresses (σ_1 and σ_3) at crown, sidewall, and floor of the circular and horseshoe tunnel geometries for granite with K=1 and K=4. Please note that the red and blue curves represent the general behaviour observed at the points from which the measurements were taken.

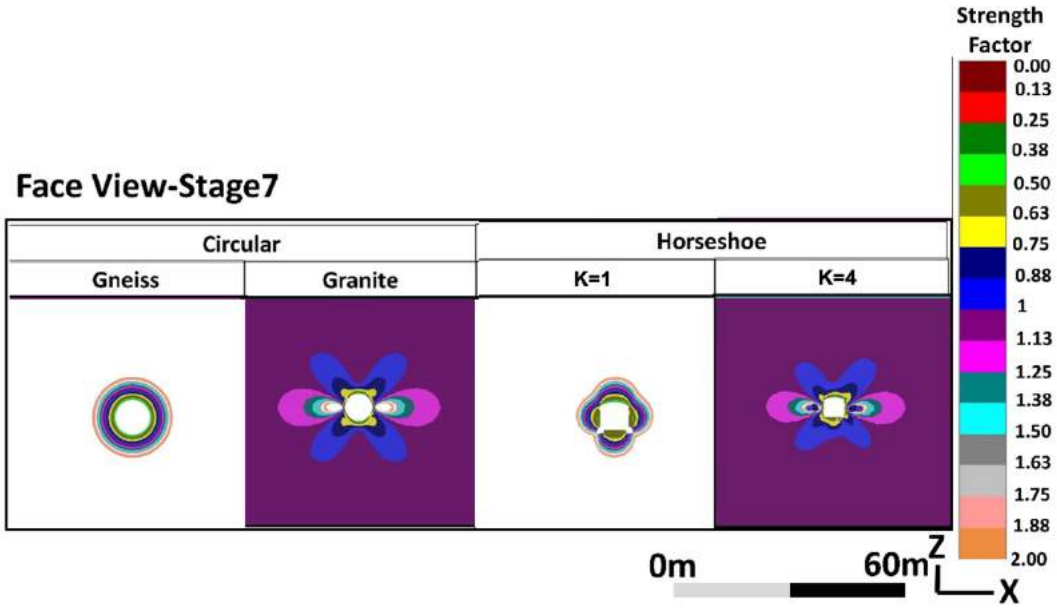

Figure 6. Numerical models representing strength factor distribution at face view for K=1 and K=4 for granite and both geometries (circular and horseshoe). Please note that the white region around models in K=1 represent higher strength factors (> 5) values than the K=4.

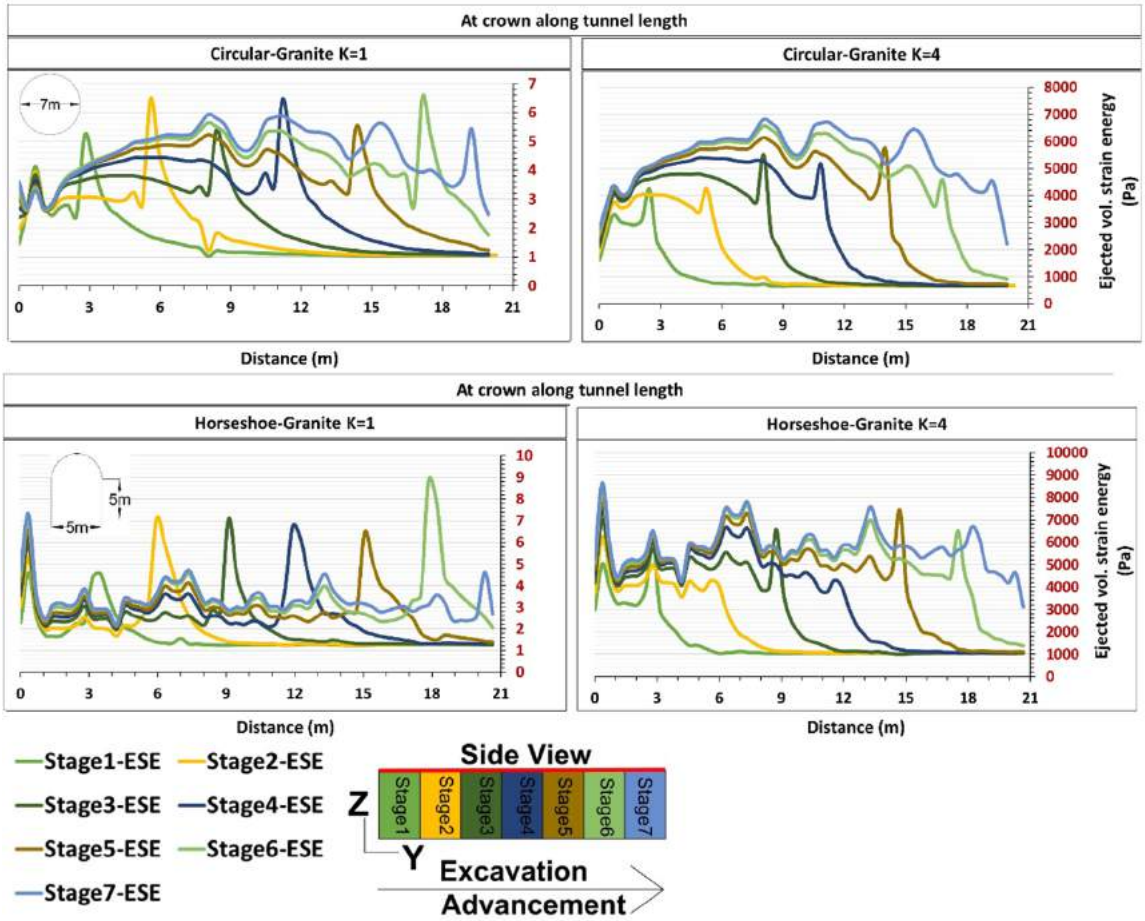

Figure 7. Elastic strain energy release of the ejected material for K equal 1, 4 for granite at the crown of the circular tunnel and at the crown of the horseshoe tunnel.

6. Concluding Remarks

This work numerically investigates the strain-bursting phenomenon occurring in deep underground environments where high stress magnitudes take place mainly in hard brittle rock materials associated with sudden energy release. From this analysis it is demonstrated that: i) the geometrical variations between the horseshoe and circular tunnels have an essential role in enhancing the energy storage, the energy release, and the extent of failure. The flat surfaces of the horseshoe tunnel cause higher energy storage and release compared to the arc surface of the crown. The circular tunnel crown and floor display nearly an equal energy response; ii) different geometries can enhance the energy storage increase with K ratio in the near field. This was noted as the horseshoe tunnel displayed a greater increase in energy storage. Additionally, the intensity of the geometry impact can be less or more with different rock masses, as it was noted that granite rock mass was more impacted by the horseshoe tunnel's geometrical differences than gneiss; and, iii) the strength factor tool in EX3 software effectively estimated the failure depth, positively correlated with semi-empirical equations introduced by [4] and [12]. Finally, this work proposes an approach that can be used for the prediction strain bursting and assessing the energy response before and after excavation.

References

[1] Paraskevopoulou, C., Cornaro, A., Admiraal, H., Paraskevopoulou, A., 2019. Underground space and urban sustainability: an integrated approach to the city of the future. *In: Changing Cities IV* Spatial Design, Landscape and socioeconomic dimensions, June 2019, Crete, Greece.

[2] Diederichs, M.S. 2003. Manuel Rocha medal recipient: rock fracture and collapse under low confinement conditions Rock Mechanics and Rock Engineering, 36 (5) (2003), pp. 339-381

[3] Kaiser, P.K., McCreath D.R., Tannant D.D. 1995. Canadian rockburst support handbook Geomechanics Research Centre and CAMIRO.

[4] Martin et al. 1999. Hoek-Brown parameters for predicting the depth of brittle failure around tunnels. Canadian Geotechnical Journal, 36 (1999), pp. 136-151

[5] Vazaios, I., Diederichs, M. S. & Vlachopoulos, N., 2019. Assessment of strain bursting in deep tunnelling by using the finite-discrete element method. *Journal of Rock Mechanics and Geotechnical Engineering,* 11(1), pp. 12-37.

[6] Diederichs, M. S. 2007. The 2003 Canadian Geotechnical Colloquium: Mechanistic interpretation and practical application of damage and spalling prediction criteria for deep tunnelling. *Canadian Geotechnical Journal,* Volume 44 (9) (2007), pp. 1082-1116.

[7] Castro, L. A., Grabinsky, M. W. & McCreath, D. R., 1997. Damage initiation through extension fracturing in a moderately jointed brittle rock mass. International Journal of Rock Mechanics and Mining Sciences, 34(3-4), pp. 110.e1-110.e13.

[8] Diederichs, M. S., 2018. Early assessment of dynamic rupture hazard for rockburst risk management in deep tunnel projects. *Journal of the Southern African Institute of Mining and Metallurgy,* Volume 118, n.3 http://dx.doi.org/10.17159/2411-9717/2018/v118n3a1

[9] Berbia, C. A., Telles, J. F. & Wrobel, L. C., 1984. *Boundary Element Techniques, Theory and Applications in Engineering*. Berlin: Springer.

[10] Mahabadi, O. K., Cottrell, B. E. & Grasselli, G., 2010. An Example of Realistic Modelling of Rock Dynamics Problems: FEM/DEM Simulation of Dynamic Brazilian Test on Barre Granite. *Rock Mechanics and Rock Engineering,* Volume 43, pp. 707-716.

[11] Villeneuve, M.C., Heap, M.J., Kushnir, A.R.L. *et al*. Estimating in situ rock mass strength and elastic modulus of granite from the Soultz-sous-Forêts geothermal reservoir (France). *Geotherm Energy* **6,** 11 (2018). https://doi.org/10.1186/s40517-018-0096-1

[12] Kaiser, P. K., 2006. Rock mechanics considerations for construction of deep tunnels in brittle rock. In: C. F. Leung & Y. X. Zhou, eds. *Proceedings 4th Asian Rock Mechanics Symposium*. Singapore,: 8–10 November 2006, pp. 47-58.